AN ESTIMATION OF VERTICAL SLOW DRIFT BETWEEN STORAGE RING AND NANOSCOPIUM LONG BEAMLINE AT SYNCHROTRON SOLEIL

A. Lestrade, C. Bourgoin, N. Jobert, N. Hubert, A. Somogyi, L. Nadolski, JC Denard, P. Eymard, M. Ros, F. Thiam, Synchrotron SOLEIL, Saint-Aubin, 91190 GIF sur Yvette, France

Abstract

Hydrostatic Levelling system and beam diagnostics have revealed vertical slow drift between Storage Ring and the long beamline at SOLEIL. An Experimental hall air conditioning effect is even the origin of the SR slab deformation at the beamline source point. We analyse the situation with metrology tools as spatial differential processing of data, metrology loop, stability time constant and by applying the heat diffusion equation to a wall. Both HLS and beam diagnostics are compared into the tunnel. The perturbations are finally analysed through the simplified optical model of the beamline.

INTRODUCTION

The highest stability, from the hundred Hertz range to the slow drift domain, is required for beamlines such as NANOSCOPIUM, dedicated to scanning hard X-ray nanoprobe techniques. Since the time span of a scan is about 8 hours, the long term stability is critical. A wide experiment at the hall scale held in spring 2014 to highlight the effect of thermal drift on the experiment stability. Measurement analysis on both, beam diagnostic and Hydrostatic Leveling System (HLS) have been realized to try to dissociate movement due to the source from the beamline slab ones. Stability has been studied according to the two following points of view, the infrastructure design of synchrotron sources and the NANOSCOPIUM optics. We formulate the optical design of the beamline, a scheme dedicated to minimize the effects of the structure instabilities on the beam position. Then, we present the HLS sensor, processing and accuracies.A model is proposed to explain the slab deformation around the straight section of the beamline source point based on the heat diffusion equation throught a wall, and finally we review the different experimental measurements held these last years.

NANOSCOPIUM OPTICAL DESIGN

The optical design (Figure 1) of Nanoscopium aims to reduce the instabilities of the probing nanobeam by creating an overfilled secondary source in both directions, and by the all horizontally reflecting main beamline optics [1] [2].

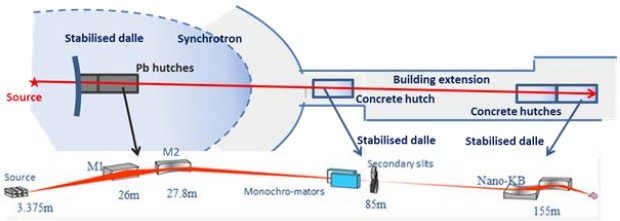

Figure 1: Optical layout of the Nanoscopium beamline.

The two mirrors, M1 and M2, are focusing the photon beam at the position of the slit secondary source (SS), with $M_v = 2.61$ (vertical) and $M_h = 2.36$ (horizontal) - magnifying geometry, for M1 (sagittal) and M2 (tangential) respectively. The size of SS is determined by a high precision slit-pair. As the SS is situated behind the main optical elements, it acts as angular stability filter; angular and positional beam instabilities will be reflected in the variation of the intensity after the SS. The stability criteria of the X-ray source and of the mirrors was defined compared to its aligned position and as causing less than $\Delta I/I < 10\%$ intensity variation over 8h at the secondary source whose vertical size is $l_S = 10\mu m$. This allows defining the overall stability requirements of the secondary source relative to the experimental stations, separately. Simulating the beam whose Gaussian profile ($fwhm = 60\mu m$), such a $\Delta I/I = 10\%$ loss of intensity corresponds to a drift of the photon beam ($h\nu$) with respect to the slit of approximately [3] $z_{h\nu/SS}$~$10\mu m$. The relative vertical position variation between photon beam and mirror will cause a vertical position change at the SS position through the vertical mirror whose magnification corresponds to the distances ration between source point, M1 and SS:

$$M_v = -\frac{D2}{D1} = -2.61 \quad (1)$$

It gives a condition on the electron beam (e^-) stability at the source point:

$$z_{e^-/M1\_SS} < \frac{1}{M_{v_1}} . z_{h\nu/SS} \sim 4\mu m \quad (2)$$

where $z_{e^-/M1\_SS}$ is defined with respect to the optical axis, i. e. the points M1 and SS.

The thin lens model can be applied to the optical function of NANOSCOPIUM to evaluate the effect of misalignments . It reveals the very low sensitivity of the

optical system to beam vertical angular deviations $z'_{e^-/M1\_SS}$ (Figure 2). But it is limited by the relative vertical direction between the electron beam and the mirror M1which induces a vertical photon beam size spread. Its acceptable limit is given to reach the $\frac{\Delta I}{I} <$ 10% condition (calculated by simulations, [3]):

$$\left|z'_{e^-/M1\_SS}\right| < 10\mu rad \qquad (3)$$

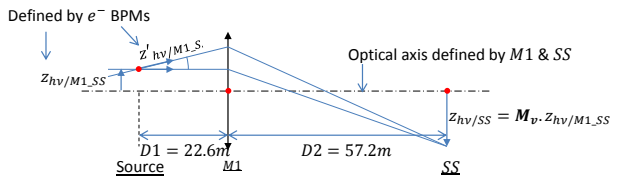

Figure 2: Only the z misalignment of the source wrt M1_SS defines the beam position at the SS location.

THE HYDROSTATIC LEVELING SYSTEM

The instrument is based on a non-contact displacement capacitive sensor [4]. The physical principle is described by two electrodes and the air in between acting as the isolator of the capacitor. One electrode is constituted by the sensor itself and the other one by the part to be measured. Since both are conductors, a capacitive charge exists between them and the corresponding voltage across the capacitor varies with their mutual distance according to the following relationship:

$$d = \varepsilon\varepsilon_r \frac{S}{C} \qquad (4)$$

S,C, ε and ε_r depict the surface of the capacitor, the measured capacitance and the dielectric constants.

High sensitivity is now reached down to the nanometer level (for a very tiny range) with the most recent models proposed by the manufacturers [5]. In the case of the HLS, the part to be measured is a conductive liquid surface, with a signal conditioning being optimized for such conditions (Figure 3)).

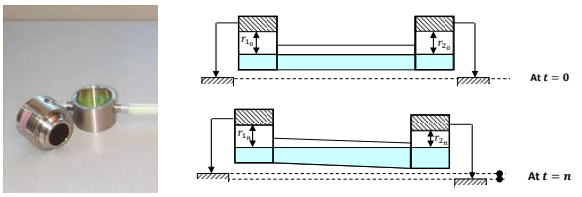

Figure 3: a) HLS sensor with vessel and pipe. b) Principle of HLS.

It is planned to equip the strategical devices all along the NANOSCOPIUM beamline with HLS sensors, from the source point to the sample station. The following devices are now equipped with HLS (Figure 4): the two straight section BPM stands since they completely define the photon source point (SP) in position, the XBPM stand, giving a first position information of the photon beam inside the SR tunnel, the M1 pre-focusing mirror marble equipped at both ends with sensors since it is sensitive to z and to longitudinal inclination and finally the marble hosting the slit defining the secondary source (SS), with three sensors for z direction.

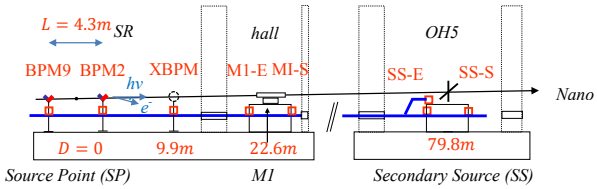

Figure 4: The NANOSCOPIUM HLS network phase n. 1.

Such a HLS network should allow to estimated relative drift of concrete slabs between the tunnel and the OH5 optical hutch, and the impact on the beam position at the SS location.

Tidal effects and stability of the surface of water

The referential of the HLS measurements varies permanently with the tides. In other words, HLS are affected by an angular common mode on the raw measurements. The amplitude of tidal effect may reach 0.2µrad, i.e. 20µm at a 100m distance. That effect must be subtracted to the sensor reading to properly interpret vertical displacements. Modelling the tides could solve the problem but it is very hard to implement [6].

Despite the fact that a liquid surface is highly instable, the HLS uses it as a measurement reference, even for high accuracy applications. The surface remains very calm if there is no mechanical perturbation. In case of mechanical perturbations, the capillary surface waves show very small amplitude at very high frequencies [7]. So, an integrated time of about 1s for the measurements is enough to cut off the perturbation. The main issue may come from the gravity regime that moves the liquid with higher amplitudes at lower frequencies [8]. Therefore, the pipes must be strongly fixed on structures and all nearby vibration sources sufficiently isolated.

A free surface is not a plane since it follows the shape of the equipotential surface of gravity [9] [10]. This is not an issue if the water surface of the HLS network is only used as a stability reference. The tides tilt the surface with respect to the gravity direction. It is treated through the spatial differential processing.

Spatial differential processing

It is easy to prove that the relative positions of several points do not depend on the definition of the referential for measurements and processing. The case of three aligned points (Figure 5) is given with the following formula and corresponds to the distance of $P3$ with

respect to a calculation reference line defined by $P1$ and $P2$. It is the so called Spatial Differential Processing (SDP):

$$z_n \sim r_n - \left(r_{1_n} + \frac{(r_{2_n} - r_{1_n})}{(L_2 - L_1)} * (L - L_1) \right) \quad (5)$$

The angle of two pairs of points are processed as:

$$z'_n = \frac{r_{4_n} - r_{3_n}}{L_4 - L_3} - \frac{r_{2_n} - r_{1_n}}{L_2 - L_1} \quad (6)$$

A temporal differential processing is then applied to study the evolutions: $z_{0n} = z_n - z_0$ and $z'_{0n} = z'_n - z'_0$.

The L_k depict the lengths between sensors along the line whose origin is located at L_1 from $P1$ and the r_{k_n} are the HLS raw readings at the time n.

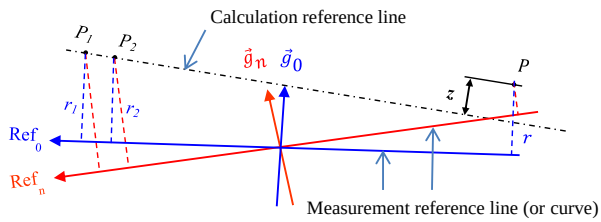

Figure 5: Spatial Differential Processing (SDP): the relative position of points do not depend on the referential

The geometrical interpretation is a displacement of the P_k with respect to the reference line. One can extend the rule to any number of sensors. As an example, we apply a reference plane through a least squares calculation to all the 168 sensors hosting the storage ring at any n discrete time as a 3D spatial differential processing [11]. From this, it is easy to calculate any relative quantity, especially the z displacement but also angular variation between structures. Between two points, the only solution is to use the HLS raw readings which can be an issue for precise displacement because the accuracy is then limited by the unknown tidal effect amplitude.

SDP eliminates tidal effects on HLS measurements. The HLS measurements must be linked to the optical scheme of the beamline to estimate the beam deviations on SS through the mirror M1 due to slow drift of slabs and structures. For this, the SDP is used with optical axis of the beamline defined above as the reference line. Applying the SDP with the HLS hosted in the BPM stands as the reference line, and the other HLS acting as $P3$ allows simulating the photon beam position variations if it were free of optics all along the beamline.

SDP can be used for other instrumentation than the HLS like the beam position monitor readings as BPM and XBPM (see Section 0). In this case, common modes due to the beam position and angle motion (z, z') can be eliminated and then, relative displacements between monitors are calculated.

It is fundamental to remind that we cannot know which part is "fixed" with respect to the ground, the displacement information remains relative.

Stability test of HLS sensors

Many experiments have been held to estimate the quality of HLS [12] [13]. One issue is their measurement electronics dependency on temperature [14]. In order to study the slow drifts of measurement systems we introduce the Stability Time Constant (STC) which is defined as the acceptable parasitic displacement δd during the time of measurement δt: $STC_{DOF} = (\delta d, \delta t)$ where DOF depicts the concerned differential degree of freedom between instrument and the object to be monitored [15] [16].

Monitoring beamline components leads to tiny displacements (few µm) and the only challenge is the stability of such sensors which must match with STC compatible with the values defined in Section 0 at SS location. The accuracy of HLS has been evaluated at SOLEIL [14]. The system shows a $STC_{HLS_{dr}} = (< 0.07\mu m\ ptp, 8h)$. Applying the HLS measurement standard deviation of $1\sigma = \frac{0.07}{4} = 0.018\mu m$ in the SDP formulaes according to the random error combination allows estimating the z and z' accuracies. Table 1 summarizes the z accuracies over 8h for two main configurations: a) the photon beam position variations if it is free of optics all along the beamline, b) the photon beam travel throught the optical scheme of the beamline and c) the relative z' accuracy between SP and M1 marble.

Table 1: z & z' HLS accuracy

Reference line	Point	σ_z (µm)	Reference line		$\sigma_{z'}$ (µrad)
a) BPMs	XBPM	0.1	c) SP (BPMs)	M1s	0.03
	M1	0.2			
	SS	0.5			
b) M1-SS	SP	0.1			

Metrology loop and parallel topology with a photon beam

As a primary outcome, we wanted to compare beam position and HLS measurements since the photon beam stability is the main topic of that study. That is the reason why the HLS sensors have been carried out as close as possible to the functional parts of the beam position monitors ($h = 364mm$) and not sealed on the floor. Figure 6 shows the corresponding metrology loop we designed. It includes mechanical links made of invar, electronics of sensors and stability references (beam and free surface of water). For this loop, any z instability of a component appears, because the sum of the measurements over the loop should be invariant in time [17] [16] [18].

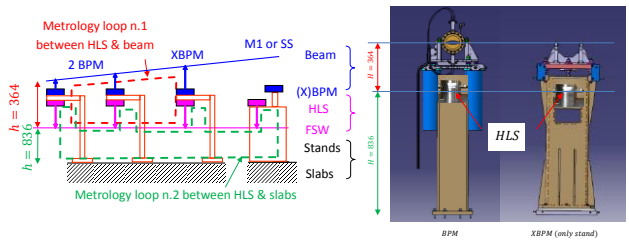

Figure 6: BPM & XBPM hosting HLS sensors and the two metrology loops

The idea is to process the set of beam monitors readings as for the HLS ones. SDP is applied in parallel to the two kinds of measurements. The SDP is applied with the BPMs as points $P1$ and $P2$ and the XBPM as $P3$. Since the water surface and the photon beam are the corresponding stability reference lines for the two measurement systems, the relative displacements of the three points must be seen identically without any common mode of the beam (as its angular and vertical motions with respect to the ground) and of the FSW (as the tides). It corresponds to the metrology loop n.1 on Figure 6 which excludes stands and ground.

An analysis of the data of June 2013 shows a correlation between beam monitoring and HLS (Figure 7) at the XBPM location, at the µm level and during 5 days. The system has been giving similar results for a couple of years.

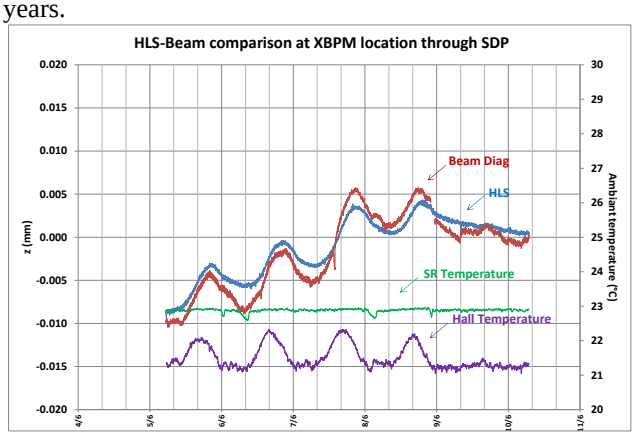

Figure 7: Beam monitors and HLS data show a strong correlation

HEAT DIFFUSION THROUGH THE SR WALL

A correlation appears through the metrology loop n.1, between the XBPM/HLS and the hall temperature. Peaks on Figure 7 show a 24h period for both instrumentations, with a time shift of about 3h between temperature and displacement quantities. HLS cannot be influenced by temperature since their electronics location is inside the SR tunnel. We can conclude it has another origin. The phenomenon has been being very regular for a couple of years.

We have developed a hypothesis to try to explain the results of the measurements [19]. The temporal temperature variation of the hall $T_h(t)$ may have an impact on the Storage Ring tunnel wall (Figure 8) through $\Delta_z T_w(t)$ the variation of the temperature between top and bottom of the wall. The upper region of the wall is more influenced by the hall temperature variations than its bottom part, which is influenced by the stable temperature of the ground and partially protected from the air conditioning by the beamline hutches around.

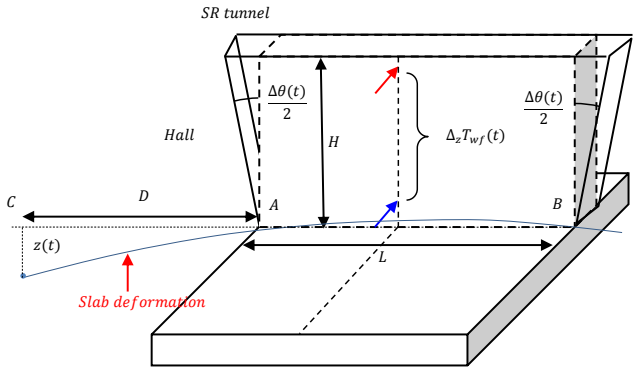

Figure 8: Hypothesis of deformation of the SR walls: the z of point C with respect to the points A & B changes with T_h the hall temperature

This temperature variation leads mechanically to a flexion of the walls (along their longitudinal direction), and consequently of the storage ring slab. The slab shows a difference slope $\Delta\theta$ between the points A and B [19]:

$$\Delta\theta(t) = \frac{\alpha L \Delta_z T_w(t)}{H} = \frac{\alpha L (T_{w,top}(t) - T_{w,bottom}(t))}{H} \quad (7)$$

where α is the coefficient of thermal expansion (CTE) of the wall material, L is the distance between A and B, and $T_{w,top}(t)$ (resp. $T_{w,bottom}(t)$) is the average wall temperature through thickness at top (resp. bottom), at time t.

Using the 1D heat equation allows to estimate the average temperature through thickness, for different hall air temperature profiles. By applying the 1D harmonic response $\omega = 2\pi/P$ since the first investigations show a periodic wave for $\Delta\theta$, we get for the heat equation [19]:

$$T_w(x,t) = T_{wf} . e^{-\sqrt{\frac{\omega}{2a}}x} . \cos\left(\omega t - \sqrt{\frac{\omega}{2a}}x\right) \quad (8)$$

Where $T_w(x,t)$, T_{wf} and a depict the wall temperature of a point whose depth into the wall is x, the wall face temperature and the diffusivity of the material. The clear bending effect on the wall will be controlled by the integral of all forces (both tensile and compressive) acting

at each elevation. For this reason, we introduce the effective temperature penetration depth, δ_{eff}, the depth defining the effective length on which the thermal forces apply. To further simplify the analysis, we correctly assume that the time-dependency is such that the penetration depth remains much smaller than the wall thickness. In such a case, the infinite 1D form of the heat equation can be used:

$$\delta_{eff}(t) \cong \sqrt{\frac{aP}{2\pi}}\sin(\omega t + \pi/4) \tag{9}$$

$$\Delta\theta(t) = \frac{\sqrt{\frac{aP}{2\pi}}\sin(\omega t+\pi/4)}{wall_{thick}}\frac{\alpha L \Delta_z T_{wf}(t)}{H} \tag{10}$$

In addition we define $z(t)$ the z variation of the point C on Figure 8: Hypothesis of deformation of the SR walls: the z of point C with respect to the points A & B changes with Th the hall temperature and $S_{z/\Delta_z T_{wf}}$ the thermal susceptibility of the straight section slab:

$$z(t) \sim \frac{\sqrt{\frac{aP}{2\pi}}\sin(\omega t+\pi/4)}{wall_{thick}}\frac{\alpha LD}{2H}\Delta_z T_{wf}(t) \tag{11}$$

$$S_{z/\Delta_z T_{wf}} = \frac{z(t)}{\Delta_z T_{wf}(t)} = \frac{\sqrt{\frac{aP}{2\pi}}\sin(\omega t+\pi/4)}{wall_{thick}}\frac{\alpha LD}{2H} \tag{12}$$

EXPERIMENTAL RESULTS

Campaign of June-July 2014

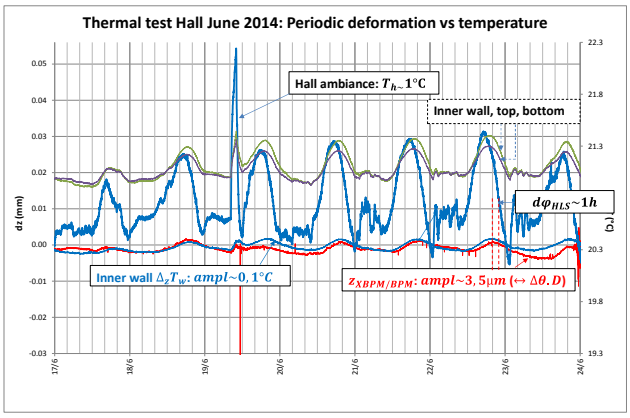

Figure 9: June 2014 measurements, harmonic response

Several sensors have been temporarily installed in the wall portion corresponding to the NANOSCOPIUM straight section. A test held in June-July 2014 during a normal beamline run of the synchrotron (Figure 9). A periodic phenomenon clearly appears with P=24h. It happens each time the weather is sunny: in that case, the air conditioning of the hall reacts by a pseudo-sine wave of about 1°C amplitude.

An analysis is done by using the amplitudes of the temperature difference $\Delta_z T_{wf}$ in (quasi) surface of the wall and of the HLS measurements at XBPM location. The link is estimated by applying Eq. 11. Then, Eq. 12 is used to estimate the slab z thermal susceptibility with respect to $\Delta_z T_{wf}$ and to HLS measurements. We have also calculated the slab z thermal susceptibility with respect to the hall temperature variations.

The calculations use the parameters of a standard concrete: $a = 0.610^{-6} m^2/s$, $\alpha = 12.10^{-6} m/°C$, a 24h period: $P = 86400s$ and the distances $H = 2m$, $D = 10m$, $L = 4.3m$.

Table 2: Results of harmonic response, June 2014

Parameter	Theoretical	Measured	Equation
$\delta_{max}(m)$	0.09	N/A	9
time shift (h)	4	<1	9
$z_{XBPM/BPM}$ (µm)	1.2	3	11
$S_{BPM_{\Delta_z T_{wf}}}$ (µm/K)	12	30	12
$S_{BPM_{T_h}}$ (µm/K)	N/A	3	N/A

Z and time shift show differences with the theory, the reality being more complex than the model. For example the signal excitation is not a pure sine wave. Nevertheless they tend to show a link between hall temperature and HLS variation at the XBPM location. In addition, it proves the existence of an inner gradient into the wall without any ambiguity.

Campaign of March 2014

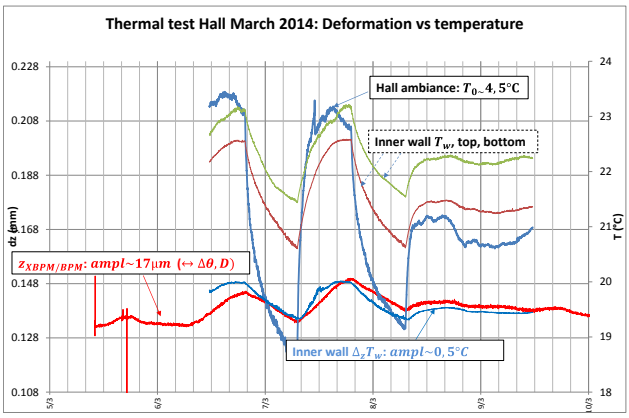

Figure 10: March 2014 measurements, step response of inner wall

In March 2014, a test at the scale of the hall has been organized (see Figure 10). The aim was to increase the daily phenomenon by doing a temperature step twice in a 24h lag. It corresponds to a step response since the set point air conditioning had been being forced at +/-2°C

suddenly. But the link between $\Delta_z T_{wf}$ and HLS cannot be considered so, because $\Delta_z T_{wf}$ is strongly attenuated and shows a pseudo-triangular signal.

The same analysis as for the June-July 2014 campaign is done by using the waves amplitude of the temperature difference $\Delta_z T_{wf}$ and the HLS measurements. The ratio between both is quite similar to the measurements of June-July 2014 and the phase shift is closed to the theoretical value of harmonic response ($d\varphi \sim 3h$). The analysis cannot go further because of the lack of measurements, the duration test being too short.

Table 3: Results of step response, March 2014

Parameter	Theoretical	Measured	Equation
time shift (h)	4	3	9
$z_{XBPM/BPM}$ (μm)	5	17	11
$S_{BPM_{\Delta_z T_{wf}}}$ ($\mu m/K$)	50	34	12
$S_{BPM_{T_h}}$ ($\mu m/K$)		3.7	12

Heat diffusion modelization have given not perfect results. However, the main question has been solved: a vertical temperature gradient variation has been identified into the wall and $Z_{BPM/XBPM}$ is clearly correlated with both, T_{hall} and $\Delta_z T_h$.

Estimation of slabs displacements

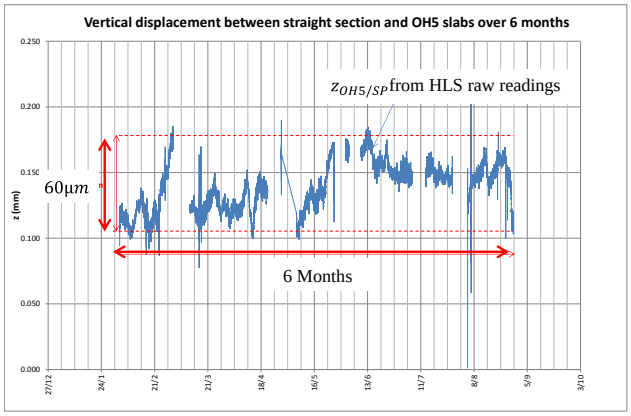

Figure 11: Vertical displacement between slabs, 60µm over 6 month, a good infrastructure design

The choice of the pair of BPMs as the reference line for HLS processing seems to be relevant for estimating the deviations of a free beam without optics at the SS location and which could correspond to slabs z displacement. But a study from Sept 2014 to Sept 2015 demonstrates that the amplitude of z variations between these slabs are more important if the HLS measurement are processed with respect to BPMs reference line than with respect to SS marble reference line. It tends to prove that the straight section z' is less stable than the SS marble one. Due to the unfavorable ratio between reference and measurement lengths (4m against 80m), any parasitic z'_{BPM}, whatever its origin (mechanics, electronics, etc.) induces a direct effect e_z on the $z_{SS/BPM}$ calculation superimposed to the true $z_{SS/SP}$ vertical displacement between slabs.

The direct use of HLS readings without SDP shows the lowest amplitude. Using directly the HLS readings remains the best approximation of slab displacements, limited to tidal effects. Figure 11 summarizes the slab displacement over a year. From the HLS readings, the slab displacement maximum amplitude is only 0.06mm over 6 months a very good result of infrastructure design.

Beam stability through NANOSCOPIUM optics

The most demanding specification of stability for the beamline users is to reach the value given in Eq. 2 at the SS location. The other constraint is to fit to Eq. 3 in terms of angular variations. The HLS monitoring of the beamline componants as BPM, M1 and SS, allows determining the beam displacements due to structures and slabs slow drift.

Figure 12 shows the HLS measurement of 3 weeks during a machine run. During that period, $z_{B/SS}$, the vertical position of photon beam varies of about 80 μm with respect to the SS. The peak to peak amplitude over a 8 hours temporal window, namely $z_{B/SS_{8h}}$ has been calculated, and 69% of resulting data are below the 10 µm tolerance. HLS measurements point out the excellent stability of the angular vertical variation of the beam with respect to M1 since its amplitude is only 3µrad over 3 weeks, corresponding to 100% success rate. A spectral analysis of the Sept 2014 data, hall temperature shows a daily peak and a smaller one with a 12h period. $z_{B/SS}$ and $z_{B/SS_{8h}}$ does not present those peaks, that should mean that there is no significant effect of hall temperature variation on z at the SS. A period from Sept 2014 to Sept 2015 is summarized on Figure 13 where appear the beam statistics at the secondary source including success rates of z position and values of z' inclination over several weeks. Notice that the curve of the z position success rate has been decreasing regularly for a year. The reason must be studied through more details.

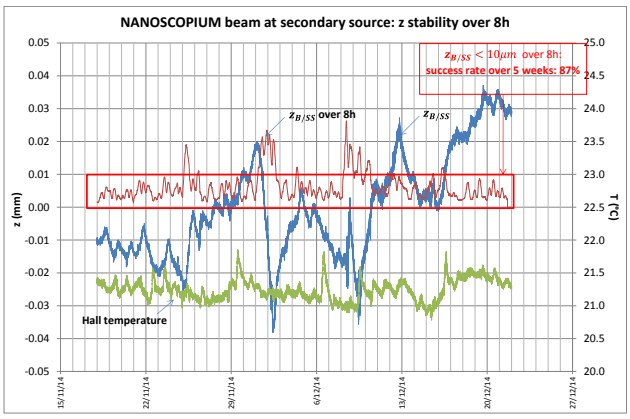

Figure 12: Beam z stability at the secondary source

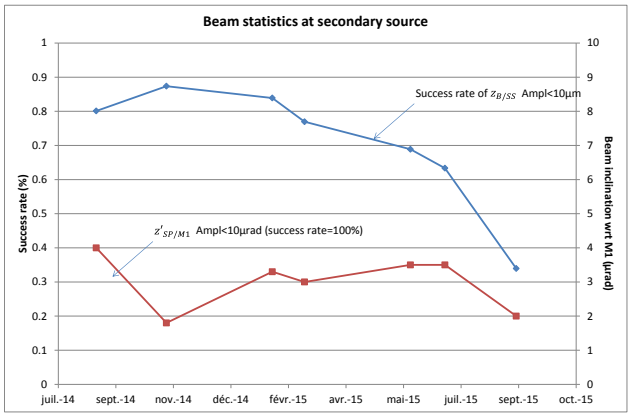

Figure 13: Statistics at the secondary source over a year

CONCLUSION

The HLS data on NANOSCOPIUM beamline have been analysed in order to estimate the infrastructure stability between the straight section defining the beamline source point and the OH5 slab hosting the secondary source. A comparison with (X)BPM beam positioning monitors shows that these instruments prove their micrometric accuracy for slow drift measurements. Periodic slab vertical movements at the beamline source point area have been detected by both instrumentations. The thermometric campaigns and the physical modeling tend to link this phenomenon to the air conditioning system variations of the Experimental Hall.

The slab z variation between straight section and OH5 is about $50\mu m$ max over a run and about $60\mu m$ over the 6 last months. The slab z' variation between straight section and OH5 is typically $1\mu rad$ over a run, and $4\mu rad$ between straight section and M1. It could mean the M1 area is the less stable.

The beam stability over 8h at the secondary source location reaches the $10\mu m$ of z requirement which corresponds to $4\mu m$ stability at the source point, with a success rate of 69% in average and is better than the $10\mu rad$ of z' requirement in 100% cases. There is no correlation detected with the hall temperature variations.

REFERENCES

[1] A.Somogyi, F.Polack and T.Moreno, "Nanoscopium: a Scanning Hard X-ray Nanoprobe Beamline at Synchrotron Soleil.," in *AIP Conference Proceedings*, 2010.

[2] Somogyi, A., Medjoubi, K., Baranton, G, Le Roux, V., Ribbens, M., Polack, F., Philippot, P and Samama, J. P., "Optical design and multi-length-scale scanning spectro-microscopy possibilities at the Nanoscopium beamline of Synchrotron Soleil," *Journal of Synchrotron Radiation,* pp. 22 (4): 1118-1129, 015.

[3] Moreno T. and Xiaohao D., "Tolerances of the two first mirrors of Nanoscopium," 2009.

[4] A. G, Les capteurs en instrumentation industrielle, Dunod, 1999, pp. 356-364.

[5] Fleming A.J., "A review of nanometer resolution position sensors: Operation and performance," *Sensors and Actuators,* vol. A 190, p. 106–126, 2013.

[6] B. J., "Analyse et modélisation de l'effet des marées sur les réseaux de nivellement hydrostatiques du CERN," Strasbourg.

[7] C. J. H. J. C. Earnshaw, "High-frequency capillary waves on the clean surface of water," *Langmuir,* vol. 7 (11) , p. pp 2419–2421, 1991.

[8] D. G. P. e. al., Gouttes, bulles, perles et ondes, Belin.

[9] W.Lowrie, Funadmentals of Geophysics, Cambridge: university of cambridge, 2007.

[10] J Boerez, "Analyse et modélisation de l'effet des marées sur les réseaux de nivellement hydrostatique du CERN," université de Strasbourg , Strasbourg, 2011.

[11] Guigné E., "Description des traitements et services du système d'acquisition HLS".

[12] H. M.-D. A. M. Andreas Herty, "TEST AND CALIBRATION FACILITY," in *IWAA 2004*, Genève, 2004.

[13] M. D, "The european synchrotron radiation facility hydrostatic levelling system twelve years experience with a large scale hydrostatic levelling system," in *IWAA 2002*, SPring-8, 2002.

[14] Bourgoin C., "Contrôle de la source secondaire de la ligne de lumière NANOSCOPIUM au Synchrotron SOLEIL," 2015.

[15] Alain Lestrade, C. Bourgoin, E.Guigné, M.Jagu, M.Sebdaoui and M.Ros, "Alignment Strategy Used for the Positioning of the Magnets and Girders," in *9th International Workshop on Accelerator Alignment*, 2006.

[16] Lestrade A., "Dimensional Metrology and Positioning Operations: basics for a spatial layout analysis of measurement systems," Bruges, 2009.

[17] S. Leleu, "contribution à l'évaluation des angles," 2000.

[18] L. Lahousse, "Contribution à la construction de machines de grande précision géométrique," 2005.

[19] N.Jobert, "estimation de la susceptibilite de la dalle de l'anneau aux fluctuations thermiques," 2015.

[20] J. Laclare, P. Thiry and C. Desailly, "Avant projet détaillé SOLEIL," 1999.